Growth, Luminescence, Selection Rules, and Lattice Sums of SiC with Wurtzite Structure

LYLE PATRICK, D. R. HAMILTON, AND W. J. CHOYKE
Westinghouse Research Laboratories, Pittsburgh, Pennsylvania
(Received 21 October 1965)

Relatively large and pure crystals of the rare 2*H* polytype of SiC (wurtzite structure) have been grown, using the method of Adamsky and Merz, with special attention to purity. Absorption and luminescence measurements (2 to 8°K) show that 2*H* SiC has an indirect energy gap of 3.330 eV, the largest yet reported for a SiC polytype. The polarized luminescence was analyzed, using group-theoretical selection rules to determine the active phonons, as Lax and Hopfield did for Ge and Si. The observed spectrum is consistent with the selection rules, provided there are conduction-band minima at the *K* positions of the Brillouin zone (two minima). Certain "forbidden" lines are found to be temperature-dependent, as a similar line is in Ge. It is proposed to extend to all SiC polytypes the lattice sum rule discussed by Brout and by Rosenstock. The 2*H* lattice sum at *K* is found to be within 2% of the cubic SiC lattice sum at *X*, even though the phonon energies measured in the luminescence spectra are quite different. As far as "trace variable" forces are concerned, SiC resembles C (diamond) more than it does Si.

I. INTRODUCTION

RELATIVELY pure crystals of 2*H* SiC have been grown, the largest of which are suitable for measurements of optical absorption and low-temperature luminescence. This rare polytype of SiC has the wurtzite structure, and was only recently discovered by Adamsky and Merz.[1] There has been no report on its properties as a semiconductor. Our measurements yield a number of energy-band parameters and phonon energies, and they show that 2*H* SiC is an indirect semiconductor[2] with an exciton energy gap of 3.330 eV, and, most probably, two conduction-band minima at the *K* positions of the Brillouin zone.

The luminescence, between 2 and 8°K, is attributed to recombination of an exciton bound to an unknown impurity (perhaps nitrogen). The initial bound state (impurity plus exciton) is known as a Lampert four-particle complex.[3] Indirect recombination requires simultaneous photon and phonon emission, as in other SiC polytypes,[4–9] but the 2*H* spectrum of phonon energies is quite different.

The intensity, temperature dependence, and polarization of certain emission lines have been interpreted, using the methods which Lax and Hopfield[10] applied to Ge and Si. The data appear to be consistent with group-theoretical selection rules only if the conduction band minima are at positions of C_{3v} symmetry (such as *K*). Results of absorption and luminescence measurements are combined to obtain the value of 3.330 eV for E_{Gx}, the exciton energy gap. This is slightly larger than the 3.265 eV of 4*H* SiC, previously the largest gap found in the SiC polytypes, but it does not fit a certain empirical relationship that is valid for seven other polytypes.[7]

A discussion of 2*H* crystal growth is given in Sec. II. The wurtzite structure and the symmetry of its Brillouin zone suggest the use of a large zone, which is introduced in Sec. III. Experimental results are given for absorption in Sec. IV, and for luminescence in Sec. V.

For indirect transitions in Ge and Si, in which the positions of the conduction band minima were known, Lax and Hopfield gave selection rules explaining the observed activity of some phonons, and the inactivity of others.[10] We do the reverse in Sec. VI, noting the absence of certain phonon lines in the 2*H* SiC luminescence, and using the group-theoretical selection rules to locate the conduction-band minima. The temperature dependence of a "forbidden" transition is explained in the same way as a similar dependence observed in Ge (Sec. VII). Transitions leaving the donor in an excited valley-orbit state are considered in Sec. VIII.

Certain lattice sums discussed by Brout[11] and by Rosenstock[12,13] are given for two SiC polytypes in Sec. IX, and it is proposed to extend the sum rule to all polytypes. Use of the sum rule makes possible a certain comparison of SiC lattice forces with those of Si and C (diamond).

II. CRYSTAL GROWTH

For many years 2*H* SiC was notable by its absence from the list of over 40 SiC polytypes.[14] It was eventually

[1] R. F. Adamsky and K. M. Merz, Z. Krist. **111**, 5 (1959).
[2] Many II–IV and some III–V compounds have wurtzite structure with a direct gap at $\mathbf{k}=0$. 2*H* SiC appears to be the first reported indirect semiconductor with wurtzite structure.
[3] M. A. Lampert, Phys. Rev. Letters **1**, 450 (1958).
[4] W. J. Choyke, D. R. Hamilton, and L. Patrick, Phys. Rev. **139**, A1262 (1965).
[5] D. R. Hamilton, L. Patrick, and W. J. Choyke, Phys. Rev. **138**, A1472 (1965).
[6] L. Patrick. W. J. Choyke, and D. R. Hamilton, Phys. Rev. **137**, A1515 (1965).
[7] W. J. Choyke, D. R. Hamilton, and L. Patrick, Phys. Rev. **133**, A1163 (1964).
[8] L. Patrick, D. R. Hamilton, and W. J. Choyke, Phys. Rev. **132**, 2023 (1963).
[9] D. R. Hamilton, W. J. Choyke, and L. Patrick, Phys. Rev. **131**, 127 (1963).
[10] M. Lax and J. J. Hopfield, Phys. Rev. **124**, 115 (1961).
[11] R. Brout, Phys. Rev. **113**, 43 (1959).
[12] H. B. Rosenstock, Phys. Rev. **129**, 1959 (1963).
[13] H. B. Rosenstock, J. Phys. Chem. Solids, Suppl. **1**, 205 (1965).
[14] R. S. Mitchell, Z. Krist. **109**, 1 (1957).

grown by Adamsky and Merz,[1] who used source materials and methods quite different from those normally used in SiC furnaces.[15] The temperature, for example, was about 1400°C instead of 2400°C.

Our crystals were grown after the fashion of Adamsky and Merz, but with greater attention to purity, as described in an appendix. The largest crystals are about 3 mm long and 0.3 mm in diameter, somewhat larger than reported in Ref. 1, and they are clear, not opaque. Thus, the improvement is not so much in size as in quality. The x-ray determination of polytype was by transmission Laue and by Weissenberg methods. Many crystals appear to be pure $2H$.

The Appendix also gives information on crystal habit and nucleation which is pertinent to a consideration of growth mechanisms. In particular, the recently proposed vapor-liquid-solid (VLS) mechanism is discussed.[16]

III. WURTZITE SYMMETRY AND THE LARGE ZONE

The symmetry of the wurtzite structure has been discussed in several papers.[17–19] We refer to those papers and to Koster's article[20] for the group-theoretical analysis and the character tables. Theoretical treatments of the phonon dispersion relations in wurtzite lattices have been given by Merten[21] and by Sullivan.[22] In this section we emphasize certain points that are important for the later analysis of selection rules. For indirect semiconductors such rules determine whether or not a particular phonon participates in absorption or luminescence processes.

SiC polytypes differ in the stacking order of double layers of atoms.[23] Using the ABC notation to indicate stacking order, wurtzite is denoted by AB, with the sixfold axis passing through the unoccupied C sites. The space group is $P6_3mc(C_{6v}^4)$. A slightly expanded notation is $AaBb$, indicating explicitly the two kinds of atoms, which form two identical interpenetrating *hcp* sublattices.

The silicon A and B sites (or carbon a and b) are not equivalent under primitive lattice translations, hence there are four atoms per unit cell, and 12 branches of the phonon spectrum in the Brillouin zone. However, time reversal, and the A and B equivalence under

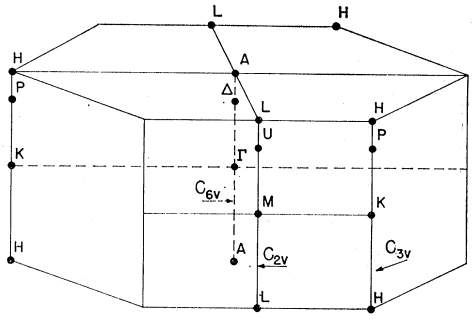

FIG. 1. Brillouin zone for the wurtzite lattice, with the standard notation for points and lines of symmetry. Three kinds of symmetry lines parallel to the axis are indicated by the corresponding point-group symbols.

screw displacements and glide reflections, result in degeneracies[24] on the planes $k_z=\pm\pi/c$. The absence of energy gaps on these planes then suggests the use of a large (Jones) zone,[25] extending to $k_z=\pm 2\pi/c$, in which there are only six branches of the phonon spectrum, three acoustic and three optic, with a considerable energy difference between acoustic and optic sets because of the large Si/C mass ratio[26] of 2.33. In the large zone only six phonons have the same wave vector $\mathbf{k}$ as a conduction-band minimum; hence six of the 12 phonons are expected to be prominent in the phonon-assisted luminescence spectrum. We have previously shown that the large-zone scheme can be used for any SiC polytype[27] and gives a simple basis for polytype comparisons.

Figure 1 shows the wurtzite Brillouin zone with the usual notation for symmetry points and lines. Some of the symmetry operators in the nonsymmorphic space group $P6_3mc$ contain nonprimitive translational components $\tau=c/2$ (c is the unit-cell height). With τ omitted, the symmetry elements form the point groups C_{6v} along Γ-Δ-A, C_{3v} along K-P-H, and C_{2v} along M-U-L, as indicated in Fig. 1. Because of the τ components, the character table for one of these symmetry lines contains complex characters $\omega=\exp(ik_z\tau)$ which depend on k_z. However, $\omega=1$ on the plane $k_z=0$, where Γ, K, and M are situated, and the characters then reduce to those of the associated point groups. Points not on the symmetry lines have, at most, reflection symmetry.

Table I gives the group characters along the Γ-Δ-A axis. The complex character ω changes continuously from 1 at Γ to i at A, at which point there are degeneracies, due to time reversal, between those representations which are complex conjugate partners at A ($k_z=\pi/c$ at A, hence $\omega=i$ and $\omega^*=-i$). Thus, there

[15] D. R. Hamilton, J. Electrochem. Soc. **105**, 735 (1958).
[16] R. S. Wagner and W. C. Ellis, Appl. Phys. Letters **4**, 89 (1964).
[17] R. C. Casella, Phys. Rev. **114**, 1514 (1959).
[18] M. L. Glasser, J. Phys. Chem. Solids **10**, 229 (1959).
[19] E. I. Rashba, Fiz. Tverd. Tela **1**, 407 (1959). [English transl.: Soviet Phys.—Solid State **1**, 368 (1959)].
[20] G. F. Koster, in *Solid State Physics*, edited by F. Seitz and D. Turnbull (Academic Press Inc., New York, 1957), Vol. 5, p. 173.
[21] L. Merten, Z. Naturforsch. **15a**, 512 and 626 (1960).
[22] J. J. Sullivan, J. Phys. Chem. Solids **25**, 1039 (1964).
[23] For polytype stacking sequences and the ABC notation see A. R. Verma, *Crystal Growth and Dislocations* (Butterworths Scientific Publications Ltd., London, 1953), Chap. 7.
[24] C. Herring, Phys. Rev. **52**, 361 (1937).
[25] H. Jones, *The Theory of Brillouin Zones and Electronic States in Crystals* (North-Holland Publishing Company, Amsterdam, 1960), Chap. 5.
[26] R. W. Keyes, J. Chem. Phys. **37**, 72 (1962).
[27] Reference 4, Sec. XV, and Ref. 5, Sec. V.

TABLE I. Group characters for $\Gamma-\Delta-A$ symmetry axis $\omega\equiv\exp ik_z\tau$, and $\tau=c/2$.

Number in class	Symmetry operator	Δ_1	Δ_2	Δ_3	Δ_4	Δ_5	Δ_6	Lattice modes	Star K
1	$\{E\|0\}$	1	1	1	1	2	2	12	2
1	$\{C_2\|\tau\}$	ω	ω	$-\omega$	$-\omega$	-2ω	2ω	0	0
2	$\{C_3\|0\}$	1	1	1	1	-1	-1	0	2
2	$\{C_6\|\tau\}$	ω	ω	$-\omega$	$-\omega$	ω	$-\omega$	0	0
3	$\{\sigma_v\|0\}$	1	-1	-1	1	0	0	4	0
3	$\{\sigma_d\|\tau\}$	ω	$-\omega$	ω	$-\omega$	0	0	0	2
Dipole moments		z				x, y			

are three degenerate pairs, A_1 with A_4, A_2 with A_3, and A_5 with A_6.

The reducible representation for the lattice modes is given in the next to last column. It is important to observe that the Si and C atoms contribute to these characters in exactly the same way, since the two sublattices differ only by a displacement along the c axis, hence transform identically under all symmetry operations. This leads to a double set of representations of lattice modes for any $\mathbf{k}$. At Γ, the irreducible representations are $2(\Gamma_1+\Gamma_4+\Gamma_5+\Gamma_6)$.[28]

The advantage of using a large zone is now illustrated by considering the phonon dispersion relations along the Γ-Δ-A axis. The phonon energy versus k_z is shown schematically in Fig. 2, in which the phonon branches go beyond A without discontinuity to $\Gamma(k_z=2\pi/c)$ at the edge of the large zone. Because of the continuous change of the character ω from 1 at $\Gamma(0)$ to -1 at $\Gamma(2\pi/c)$, the phonon branch starting as Γ_1 becomes Γ_4 for $\mathbf{k}=2\pi/c$. The representations, however, refer to the Brillouin zone, and the $\mathbf{k}$ (or ω) values are the same in both schemes only as far as A. The part beyond A is displaced by the reciprocal lattice vector $2\pi/c$ in the Brillouin zone scheme, which changes the sign of ω at A, corresponding to a switch from A_1 to A_4. The direction of increasing $\mathbf{k}$ also changes at A. Thus, the highest branch in Fig. 2 has the rather complex pattern of representations shown. In the same way, the doubly degenerate branch starting as Γ_5 at $k=0$ goes over into Γ_6 at $\mathbf{k}=2\pi/c$. The two equivalent *sets* of representations are called the acoustic and optic sets. There are three branches in each set in the large zone (counting degeneracies). This is more convenient than the three acoustic and *nine* optic branches of the Brillouin zone.

The phonon wavelength at $\Gamma(2\pi/c)$ is $\lambda\equiv 2\pi/k=c$, hence the A and B atoms (or a and b atoms), with a separation of $c/2$, are just 180° out of phase. For this reason Γ_4 and Γ_6 have been called "difference" modes by Sullivan[22] to distinguish them from the "sum" modes Γ_1 and Γ_5, in which the A and B atoms are in phase. In the Brillouin zone scheme the phonon branches are folded back at A, and the four representations appear together, whereas the large zone separates them in a natural way, "sum" at $\Gamma(0)$, "difference" at $\Gamma(2\pi/c)$. Similar relations exist along the other symmetry lines, M-U-L and K-P-H, but before reaching $k_z=2\pi/c$ these lines cross energy discontinuities at $\{10\bar{1}1\}$ planes.[29]

The six phonons with the same wave vector as a conduction band minimum in the large zone have been called the *principal* phonons.[30] In the Brillouin zone scheme, an equivalent way of explaining their prominence would be to say that the principal phonons have the same sum or difference symmetry as the electron wave function at the conduction band minimum.

IV. EXPERIMENTAL RESULTS—ABSORPTION

The weak absorption edge of indirect semiconductors makes long light paths desirable. With our samples it is necessary to shine the light along the crystal axis, which is the c axis, hence all absorption measurements

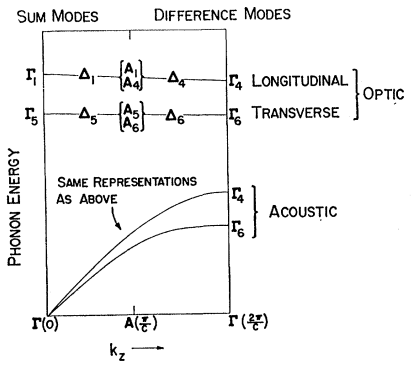

FIG. 2. Schematic phonon dispersion relations along the $\Gamma-\Delta-A$ axis in the large zone, showing how the "sum" representations at $\Gamma(0)$ go over into the "difference" representations at $\Gamma(2\pi/c)$, at the edge of the large zone. Acoustic branches have the same set of representations as the optic branches, and there are three acoustic and three optic phonons for a given wave vector $\mathbf{k}$. By folding back at A (π/c) one obtains twelve branches in the reduced zone, of which nine would be called optic. The large-zone splitting of acoustic and optic groups is more convenient, and is used throughout this paper.

[28] In the wurtzite literature there is considerable variation in the notation for representations. We follow Koster's article, in which the σ_v of the point group (Table XXIV) become mirror reflections of the space group, and the σ_d become glides (Table XXXVI). Sullivan follows Casella, who refers to Koster, but takes the σ_v as glides. This change is equivalent to an interchange of Γ_3 and Γ_4 representations. Rashba uses a notation which differs from Koster's in an interchange of Γ_5 and Γ_6.

[29] Reference 25, p. 192.

[30] Reference 4, Sec. VI.

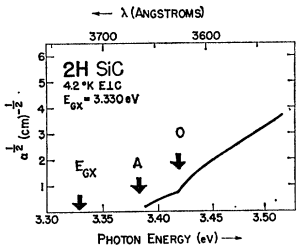

FIG. 3. Absorption edge of 2*H* SiC at 4.2°K, for light polarized $E \perp c$. The plot of $\alpha^{1/2}$ against photon energy is conventional for indirect transitions. The arrows marked *A* and *O* show the energies of the two breaks observed in the transmission curve. These breaks are thought to indicate the beginning of absorption with emission of a 52.5-meV acoustic phonon (A) or a 93.2-meV optic phonon (O), the precise energies being obtained from the luminescence spectrum. From this fit is obtained the exciton energy gap, $E_{GX}=3.330$ eV.

are for light polarized $E \perp c$. The available sample lengths are still very much less than needed for accurate measurements.[31] We would also prefer larger sample diameters than 0.3 mm, as the very narrow light beam is difficult to hold steady for measurements in the helium Dewar. To increase the stability, a servomechanism was designed to position a lens in such a way as to compensate for crystal motion, keeping the light beam constant on the slits of the monochromator.

A plot of transmitted light against phonon energy shows only two clear breaks, one at the beginning of absorption, and another 35 or 40 meV higher in energy. At the low temperatures used (4.2°K) these indicate energies at which excitons can be formed with simultaneous phonon *emission*. Without larger samples a measurement of the weak phonon *absorption* part of the spectrum is out of the question, as the structure washes out entirely at higher temperatures. We have therefore used phonon energies found in the luminescence spectrum (Sec. V) to interpret the absorption measurements. It is most plausible that the beginning of absorption corresponds to emission of the smallest acoustic phonon (52.5 meV), and the second break to the beginning of emission of optic phonons (93.2 meV). A rough agreement between absorption and luminescence data is obtained in this way, as shown in Fig. 3. We plot, as usual, the square root of the absorption coefficient against photon energy.[32] Because of the small sample size we did not measure the absolute transmission, but only its variation with wavelength. The absorption coefficient was set to zero for photon energies below the first break in the transmission curve.

The exciton energy gap E_{4x} is found to be 3.330 eV, with an uncertainty of perhaps 5 meV. This is slightly higher than the 4*H* gap of 3.265 eV, previously the largest found in the SiC polytypes. The 2*H* gap does not maintain the linear relationship found for the energy gaps of seven other polytypes as a function of percentage of "hexagonal" layers, and shown in Fig. 3 of Ref. 7. The energy gap apparently depends on the positions of the conduction band minima, which change from one polytype to another because they lie on the large zone boundary, a boundary determined by the crystal structure. Thus, there does not seem to be any good basis for the linear relationship of Ref. 7, and its failure for 2*H* SiC is not surprising.

The absorption edges previously given for SiC polytypes could be approximately superposed after an energy shift required by the differences in energy gaps, and a scale change required by the differences in absorption strengths.[33] This is a consequence of the nearly identical principal phonon energies in those polytypes. However, the 2*H* phonon energies are different, and no superposition is possible. Thus, it is more difficult to compare absorption strengths, but it is clear, nevertheless, that 2*H* is weakest of all. Values of α at equal distances from the edge are roughly one-quarter those of cubic or 15*R* SiC, and an even smaller fraction of the α's of other polytypes. This probably means that 2*H* has a small density of conduction-band states, as discussed in Ref. 4. One factor in this density is the number of conduction-band minima, which, in Sec. VI, we deduce to be only two for 2*H*, as compared with three for cubic, and six or twelve for the other polytypes.

V. EXPERIMENTAL RESULTS—LUMINESCENCE

The luminescence spectra of ZnS, CdS, and other materials with wurtzite structure have been studied extensively, and have contributed greatly to our knowledge of excitons[34] and exciton complexes,[35] but only *direct* transitions have been observed, requiring a knowledge of the band structure only at $\mathbf{k}=0$. The *indirect* transitions of 2H SiC make its luminescence spectrum more like those of Si[36] and Ge,[37] in which phonon emission plays a vital part in conserving crystal momentum. However, unlike the optically isotropic Si and Ge, 2H SiC has two distinct spectra, for electric vector parallel ($E \| c$) or perpendicular ($E \perp c$) to the optic axis (c axis). Certain intermediate states are available in each polarization direction, and it is their symmetry which determines the selection rules. Thus, for example, a certain phonon may be active in the $E \perp c$ spectrum but not in the $E \| c$ spectrum.

The crystal size was adequate for luminescence measurements, and the equipment used was the same as previously described.[38] Exploratory measurements

[31] The longest samples are tapered, and cropping the narrow end reduces the length from about 3 to 2 mm. The crystal then roughly covers the "1" printed here.

[32] T. P. McLean, in *Progress in Semiconductors*, edited by A. F. Gibson (Heywood and Company, Ltd., London, 1960), Vol. 5, p. 55.

[33] Reference 4, Sec. V.

[34] J. J. Hopfield and D. G. Thomas, Phys. Rev. **122**, 35 (1961).

[35] D. G. Thomas and J. J. Hopfield, Phys. Rev. **128**, 2135 (1962).

[36] J. R. Haynes, M. Lax, and W. F. Flood, in *Proceedings of the International Conference on Semiconductor Physics, Prague, 1960* (Academic Press Inc., New York, 1961), p. 423.

[37] J. R. Haynes, M. Lax, and W. F. Flood, J. Phys. Chem. Solids **8**, 392 (1959).

[38] W. J. Choyke and L. Patrick, Phys. Rev. **127**, 1868 (1962), and Ref. 7, Sec. III.

were made on about 20 crystals, using a grating spectrograph with Kodak 103a-0 plates. Detailed measurements were made on three crystals using a Fastie-Ebert monochromator with photon-counting equipment.

Some impure crystals have broad-band spectra which we cannot interpret. The better crystals have a line spectrum, part of which is shown in Fig. 4. Only one such spectrum was found, and all lines appear to have the same relative strength in all crystals. We therefore conclude that a single impurity is responsible for this characteristic bound-exciton spectrum. The lines shown are the one-phonon lines. Not shown in Fig. 4 is a weak no-phonon line at 3.320 eV. Also not shown, at energies below 3.2 eV, are a number of lines which appear to be two-phonon lines, and/or one-phonon lines for transitions that leave the impurity in an excited state. Such lines are not considered further. Notably absent for $2H$ SiC is the three-particle spectrum observed for many SiC polytypes.[4]

The presence of the no-phonon line indicates that the exciton is bound to an impurity, but the displacement of this line from $E_{Gx}=3.330$ eV gives a value of only 10 meV for the binding energy (E_{4x} of Ref. 4). The low intensity of the no-phonon line is a consequence of weak binding in indirect semiconductors. This, together with the disappearance of the spectrum at about 20°K, tends to confirm the small value of E_{4x}, which is uncertain to the same extent as E_{Gx}, being measured *from* E_{Gx}. Such consistency supports the value given for E_{Gx}, which was dependent on the much less precise absorption measurements, and enables us to place an error limit of about 5 meV on E_{Gx} or E_{4x}.

A value of 10 meV is near the low end of the range of E_{4x} values found in other polytypes, and suggests a *shallow* impurity, in spite of some doubts about the use of Haynes' rule for SiC.[39] The only *known* shallow impurities in SiC are the donor N and the acceptor Al, and evidence given in Sec. VIII appears to favor nitrogen.

The lines which are shown in Fig. 4 fall into three sets which can be described as follows for the $E\perp c$ spectrum. (a) There are five strong lines (numbered), of which 1 and 2 are displaced from the no-phonon line by 52.5 and 61.5 meV (in the acoustic range),[40] and 4, 5, and 6 are displaced by 91.2, 100.3, and 103.4 meV (in the optic range). (b) There are five weaker lines (primed numbers) which echo the strong lines, with a further displacement to lower energies of 5 meV. (c) There are several still weaker lines marked with lower case letters.

For the $E\|c$ direction, the spectrum is similar except that the 52.5- and 103.4-meV lines are reduced by about a factor 10. These lines are also temperature dependent, as discussed later. We interpret them as forbidden lines, and it is this that enables us to determine the positions of the conduction-band minima.

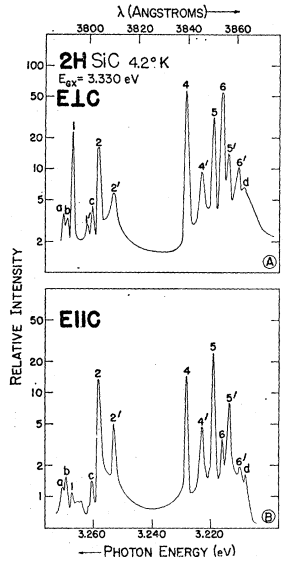

FIG. 4. One-phonon lines in the luminescence spectrum of $2H$ SiC at 4.2°K, for light polarized $E\perp c$ (top half) and $E\|c$ (bottom half). The spectrum is that of a bound exciton (Lampert complex), with a no-phonon line off scale at 3.320 eV, which is the zero for a measurement of phonon energies. From the five strong numbered lines 1, 2, 4, 5, and 6 are obtained phonon energies 52.5, 61.5, 91.2, 100.3, and 103.4 meV, respectively. Lines 1 and 6 are much reduced in the $E\|c$ spectrum. The weaker primed lines are displaced an additional 5 meV with respect to the strong lines. Other weak lines are called *a*, *b*, *c*, and *d*. The lines all fall into two groups on the basis of phonon energy. These groups are, in the large-zone terminology, acoustic at the left of Fig. 4, optic at the right.

VI. SELECTION RULES, AND LOCATION OF THE CONDUCTION-BAND MINIMA

The mechanism of exciton recombination for an indirect semiconductor is illustrated schematically in Fig. 5. For a *bound* exciton, the hole at $\mathbf{k}=0$ and the electron at $\mathbf{k}=\mathbf{k}_{CB}$ may recombine without phonon emission in some fraction of the transitions.[41] In other cases crystal momentum is preserved by emission of a phonon which either scatters the electron to an intermediate conduction-band state at $\mathbf{k}_0$, or scatters the hole to an intermediate valence-band state at $\mathbf{k}_{CB}$. Many recombination channels are available, because either the electron or the hole scattering may be to one of several bands of intermediate states. Those bands are favored which most nearly conserve energy in the intermediate state.[32]

Symmetry determines which intermediate states may be reached by optical transitions, and which phonons may participated in the scattering. For Ge and Si the

[39] J. R. Haynes, Phys. Rev. Letters 4, 361 (1960). The rule relates E_{4x} to the donor ionization energy E_i. Its applicability to SiC donors is discussed in Ref. 5, Sec. III.

[40] In other SiC polytypes, many acoustic phonons have been observed with energies below 79.4 meV, and optic phonons have fallen in the rather narrow range 94.4 to 104.2 meV. The terms acoustic and optic refer to the phonon branches in the *large* zone.

[41] In SiC polytypes with multiple donor sites, the relative strength of a no-phonon line shows a direct correlation with the binding energy E_{4x}.

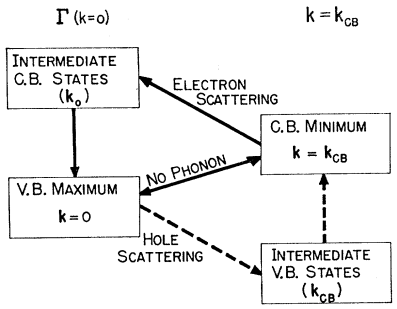

FIG. 5. Schematic of indirect exciton recombination for a semiconductor with valence band (V.B.) maximum at $\mathbf{k}=0$ and conduction band (C.B.) minimum at $\mathbf{k}=\mathbf{k}_{CB}$. The no-phonon transition occurs only for bound excitons. Other recombination modes require both an optical (vertical) transition and an electron or hole scattering, going through a number of intermediate states in which energy need not be conserved. Such states are specified in Fig. 6 for a conduction-band minimum at K.

selection rules have been discussed by Elliott and Loudon,[42] and by Lax and Hopfield.[10] The effect of time reversal has been considered by Lax.[43,44] The Ge and Si difficulties with boundary points do not occur for the wurtzite structure, which is equivalent to a symmorphic structure as far as representations are concerned.[17] For scattering between $\mathbf{k}=0$ and $\mathbf{k}=\mathbf{k}_{CB}$, the intersection group to be considered is just the group of the wave vector $\mathbf{k}_{CB}$, whose representations are simply related to those of the corresponding point group. Furthermore, initial and final states are inequivalent in this case, so that time reversal does not introduce any additional restrictions.

Our basic assumption is that the valence band structure at $\mathbf{k}=0$ is similar in all SiC polytypes. The observed polytype differences are attributed to differences in the positions of the conduction-band minima, which are at the zone boundary; hence they necessarily depend on the polytype structural differences. Thus, we assume that the representation of the valence band maximum is Γ_5, as it seems to be in other hexagonal polytypes[45] (Λ_3 in rhombohedral polytypes). We use the single-group representations because the spin-orbit splitting is small,[46] and the crystal group rather than the impurity group because the exciton binding to the impurity is weak.

We first show (Sec. VI A) that the experimental results indicating one forbidden optic phonon for $E\|c$ can be explained by conduction band minima at positions K. Then we show (Sec. VI B) that these results cannot be explained by conduction-band minima having any of the other symmetry types present in the wurtzite Brillouin zone.

A. Selection Rules at K

No assumption need be made about the conduction band representation at K, but a sketch of the band structure for the empty wurtzite lattice,[47] and a calculation of the band structure for ZnS by Herman and Skillman,[48] both indicate that the representation is likely to be K_2. No band structure calculation has been published for any SiC polytype except cubic.[49]

To obtain the selection rules, the Γ and K character tables are needed. The former is obtained from Table I by substituting unity for each ω. Table II gives the

TABLE II. Group characters at K.

Number in class	Symmetry operator	K_1	K_2	K_3
1	$\{E\|0\}$	1	1	2
2	$\{C_3\|0\}$	1	1	−1
3	$\{\sigma_d\|\tau\}$	1	−1	0
Dipole moments		z		x, y

characters at K, which are those of the point group C_{3v}, and which are used for both conduction-band and phonon representations. At K the reducible phonon representation shown in Table I reduces to $2(K_1+K_2+2K_3)$. K_1 and K_2 transform like sum and difference modes, respectively, but K_3 cannot be characterized in this way. Since optic and acoustic phonon representations are identical (Sec. III) the optic phonons alone are $K_1+K_2+2K_3$. These divide once more, into sets of principal and weak phonons. For a K_2 conduction band minimum the division is K_2+K_3 for principal optic phonons, and K_1+K_3 for weak optic phonons.

The left column in Fig. 6 shows the Γ_5 valence band maximum and possible intermediate states at Γ, with the permitted polarization of optical transitions from Γ_5. Similarly, the right column shows possible intermediate valence band states at K, and the polarization for transitions from a K_2 conduction band minimum (for which a dipole transition to a K_1 state is forbidden). The allowed phonon representations for each intermediate state, listed in the center column, are obtained by taking direct products of initial and final electron or hole representations. For example, phonons participating in hole scattering from Γ_5 to K_3 are given by

$$\Gamma_5\times K_3=K_3\times K_3=K_1+K_2+K_3,$$

since Γ_5 becomes K_3 in the intersection group.

[42] R. J. Elliott and R. Loudon, J. Phys. Chem. Solids **15**, 146 (1960).
[43] M. Lax, Phys. Rev. **138**, A793 (1965).
[44] M. Lax, *Proceedings of the International Conference on the Physics of Semiconductors, Exeter* (The Institute of Physics and the Physical Society, London, 1962), p. 395.
[45] Reference 38, Fig. 8. This discussion, for $6H$, is also applicable to $4H$.
[46] Reference 4, Sec. XIII.
[47] Reference 18, Fig. 4.
[48] F. Herman and S. Skillman, in *Proceedings of the International Conference on Semiconductor Physics, Prague, 1960* (Academic Press Inc., New York, 1961), p. 20.
[49] F. Bassani and M. Yoshimine, Phys. Rev. **130**, 20 (1963).

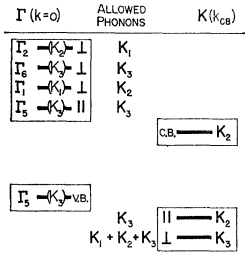

FIG. 6. Schematic like Fig. 5, but with states specified at Γ and K. States listed have representations which permit optical transitions from a Γ_5 valence band or a K_2 conduction band. At the left are shown the Γ representations and the corresponding representations in the intersection group (group of K), with polarization (|| or ⊥) of the permitted optical transition. At the right the intermediate states at K are shown in the same manner. The middle column shows the allowed phonon representations, obtained from the direct product of initial and final representations of scattered electrons or holes, using the rules $K_1 \times K_i = K_i$, $K_2 \times K_2 = K_1$, $K_2 \times K_3 = K_3$, $K_3 \times K_3 = K_1 + K_2 + K_3$.

It is observed that all phonons are permitted for $E \perp c$, but only K_3 for $E \| c$. It is clear also that some of the intermediate states can be omitted.[50] A similar analysis shows that the selection rules remain the same with a K_1 conduction-band minimum, but that there are no forbidden phonons in either polarization direction for a K_3 conduction-band minimum. Even with a K_2 or K_1 minimum the forbidden $E \| c$ phonons become permitted if spin-orbit mixing of states is introduced by use of the double groups, but this relaxation of the rules should be small in SiC. Although the "forbidden" lines have some strength in Fig. 4, their temperature dependence suggests a different reason for their presence, as explained later.

It might seem that there would be only one optic phonon line for $E \| c$, since K_3 is the doubly degenerate representation for modes with their atomic displacements perpendicular to the c axis. However, with the propagation vector also perpendicular to the c axis, K_3 represents a transverse mode and a longitudinal mode, and the two are separated in energy by the Coulomb field, which actually *reduces* the symmetry, since it is not present in the undisturbed crystal. A correlation with the observed optic phonon lines now shows that we may label those lines as TO_1 (91.2 meV), LO (100.3 meV), and TO_2 (103.4 meV), the first two being K_3 and the third K_2 (if the conduction-band minimum is K_2). The line d may possibly be one of the three expected weak lines.

As mentioned before, the acoustic phonons have the same representations, hence the same selection rules. The 52.5-meV line is apparently the K_2 line, forbidden for $E \| c$. However, there is only one other strong line, instead of two. The missing line is part of K_3, and its absence cannot be explained by group theory unless the Coulomb splitting is too small to be observed in the acoustic branch. The 61.5 meV line is broader than any of the other lines, but we were unable to split it, even at 2°K. Another possibility is that there is a physical reason[51] for the weakness of one of the lines, so that the "missing" line may be, for example, the line c. In any case there are also two or three weak lines which apparently belong to the set $K_1 + K_3$ of weak acoustic lines. However, their intensities were not sufficient for good polarization measurements, hence we cannot use these lines to test the selection rules.

For other points along the K-P-H axis, the character table is similar to that for K, but, like Table I, it has complex characters ω in the column where the mixed symmetry operator $\{\sigma_d|\tau\}$ appears. Since this change occurs in both conduction band and phonon representations, the selection rules remain unchanged. The data are therefore consistent with positions of the minima anywhere along this line. In wurtzite, however, there is no reason to expect a minimum except at points determined by symmetry,[52] and Rashba shows[19] that $\nabla_k E$ vanishes only for representations K_1, K_2, and H_3. At H there would be a degeneracy between the six principal phonon energies and the other six, hence we must exclude H if two or more of the weak lines a, b, c, and d are interpreted as phonon lines. This leaves only K_1 and K_2 as satisfactory conduction band minima (along this line of symmetry), with the empty lattice band structure suggesting K_2.

We show next that none of the other symmetry lines or planes give selection rules consistent with the experimental data, hence that the only probable representation for a conduction band minimum is K_2.

B. Selection Rules Elsewhere

As pointed out in the last section, the selection rules are independent of k_z on the line K-P-H. The same argument applies equally well to the symmetry lines Γ-Δ-A and M-U-L, hence the selection rules for these lines may be obtained at Γ and M, where the character tables reduce to those of the point groups C_{6v} and C_{2v}.

At Γ (and along Γ-Δ-A) the transverse modes are degenerate and in this case there is no lifting of the degeneracy. The presence of three strong optic lines (for $E \perp c$) therefore rules out a conduction band minimum along this symmetry line.

At M it is necessary to use the C_{2v} character table[53] and to consider schemes like that of Fig. 6, trying various M representations for the conduction band minimum, but using the same Γ levels as in Fig. 6. The

[50] Any Γ_2 state, for example, is likely to be high in energy, contributing little to the luminescence. However, omission of Γ_2 does not change the selection rules.

[51] The longitudinal acoustic phonon in Si is allowed by selection rules, but is not observed. In Ref. 44 Lax discusses the need for a physical, rather than a group theoretical, explanation.

[52] In many SiC polytypes, the planes of energy discontinuity within the large zone probably have much to do with the positions of the conduction-band minima. See Ref. 6, Sec. II.

[53] Reference 20, Table V, p. 182. Note that the numbering of the representations does not follow the order in which they are listed.

phonon modes at M are $2(2M_1+M_2+M_3+2M_4)$ in Koster's notation. For any conduction band representation, and whether all or only a few intermediate states are used, the result found is that each phonon mode may occur for $E\perp c$ or $E\|c$ but not for both. Hence the experimental data rule out the position M and any position on M-U-L.

For a conduction band minimum at a general point in the Brillouin zone there is only one representation; hence all optical transitions and all phonon scatterings are permitted. For a minimum on a reflection plane there are two representations, but it is easy to show that phonons of either representation are allowed in both polarization directions. The results are summarized in Table III. Only for K minima is the spectrum of

TABLE III. Selection-rule summary, assuming a Γ_5 valence-band maximum.

Symmetry of conduction-band minima		Selection rules for scattering
None		No restrictions
C_s	Mirror or glide plane	No restrictions
C_{2v}	$M-U-L$	Each mode in $E\perp c$ or $E\|c$
C_{3v}	$K-P-H$	One mode forbidden in $E\|c$ for P_1 or P_2 No restrictions for P_3
C_{6v}	$\Gamma-\Delta-A$	Not needed (transverse modes degenerate)

Fig. 4 explained. The reducible representation for the star of K is given in the last column of Table I. One obtains Γ_1 and Γ_3 for the two valley-orbit states of a donor.

VII. MEASUREMENTS AT 8°K

Some luminescence measurements were made with the samples *immersed* in He at 2°K and at 4.2°K. Others were made with the samples not immersed, in which case they reached a temperature of perhaps 8°K under the intense uv illumination.[54] At the higher temperature there are two striking changes in the spectrum: (a) The "forbidden" phonon lines in the $E\|c$ spectrum have approximately double their 4.2°K intensity, and (b) the five primed lines of Fig. 4 are much broader, although their integrated intensity does not change much. We interpret (b) as lifetime broadening of the final state.[55] The possible excited final states of the transition are considered in Sec. VIII. We return now to the temperature dependence of the forbidden phonon lines.

Our discussion of selection rules showed that the prohibition of K_2 (and K_1) phonons in the $E\|c$ spectrum holds for the K-P-H symmetry line, but not for $\mathbf{k}$ on the glide plane or at a general point *off* the symmetry line. Thus, the selection rule is relaxed when the thermal energy gives electrons components of $\mathbf{k}$ away from the line K-P-H. Consequently, the relative strength of the forbidden lines should increase with increasing temperature, as observed.

A similar case, for the forbidden TA phonon line in Ge, is discussed by Lax and Hopfield.[10] In the Ge luminescence, the TA line is observed, and found to have an intensity proportional to the temperature, which, as nearly as we can tell, is the dependence on temperature that we see for the two forbidden SiC lines. Macfarlane *et al.*[56] showed that the Ge absorption edge, for TA phonon emission, has the shape expected for a forbidden transition. Our samples, however, are much too small for the accurate measurements necessary to obtain such a result in the $2H$ SiC absorption.

VIII. EXCITED FINAL STATES

In this section we consider the primed lines of Fig. 4, which apparently are due to transitions to an excited final state 5 meV above the ground state. An interpretation of these lines suggests that the impurity is probably nitrogen.

The usual hydrogenic excited levels of a shallow donor or acceptor have an excitation energy comparable with the ionization energy, which, for SiC polytypes, is in the neighborhood of 0.1 or 0.2 eV.[57] The only expected states with an excitation energy of the order of 5 meV are (a) an acceptor with hole from the second valence band (energy determined by the spin-orbit effect), or (b) a donor with electron in the higher of the two valley-orbit states.

The value of 5 meV is within experimental error of the 4.8 meV found for valence-band spin-orbit splitting[46] in several other polytypes.[58] However, the only known shallow acceptor in SiC is Al, and we have seen spectra due to four-particle Al complexes in other polytypes[59] without observing a second set of lines like those under discussion here. Since the valence-band structure is thought to be very similar in all polytypes, it is hard to account for a marked difference in the Al spectrum of $2H$ SiC.

On the other hand, considerable variation in donor (nitrogen) properties in different polytypes is observed, as expected because of the variation in the position of the conduction band minima. Hence we think the impurity is likely to be a shallow donor, and nitrogen is the only known shallow donor. The only previous

[54] For relatively large $6H$ samples under similar conditions the temperature was estimated to be 6°K in Ref. 38, Sec. III. The small $2H$ samples probably reach a higher temperature.

[55] If these five lines were due to a second impurity, the energy displacement of 5 meV would indicate a stronger binding of the exciton, and the lines would be stable to higher temperatures than the unprimed lines.

[56] G. G. Macfarlane, T. P. McLean, J. E. Quarrington, and V. Roberts, Phys. Rev. **108**, 1377 (1957).

[57] Reference 4, Sec. XII.

[58] This value was determined by the observation of thermally excited states of the four-particle complexes in several polytypes. Such states could not be seen in the $2H$ spectrum because of the greater thermal instability of the $2H$ complexes.

[59] Unpublished measurements.

observation of a comparable second set of lines in a four-particle spectrum was for nitrogen in cubic SiC.[60] Their intensity, however, was only about 3% of the principal lines, instead of the 30% observed here.

We conclude that for 2*H* SiC the exciton recombination probably takes place at a nitrogen donor, and that in about 30% of the transitions the final state is one in which the donor electron is apparently in the higher of the two valley-orbit states.[61] We cannot explain why a similar process occurs in only 3% of the transitions in cubic SiC, and in an unobservably small percentage in the other polytypes.

IX. LATTICE SUMS

Although the symmetry of zincblende (sphalerite) is quite different from that of wurtzite, the two structures have much in common from a tight-binding point of view, and a number of binary semiconductors are found in both forms. This has led to comparisons of their band structures,[62] optical spectra,[63] elastic properties,[64] and lattice dynamics.[21,22] The SiC polytypes with these structures (2*H* and cubic) have quite different phonon energies for indirect transitions, a consequence of their different symmetry, but quite similar lattice dynamics according to a test we make here by summing over vibrational modes. For SiC it is natural to extend the lattice sum test to all polytypes.

For lattice vibrations in structures with two atoms per unit cell, Brout[11] has given the sum rule

$$\sum \omega_i(k)^2 = \text{const.} = ar_0/\beta\bar{M},$$

where a is a constant, dependent on the lattice structure, r_0 is the interatomic distance, β is the compressibility, and $\bar{M}$ is the reduced mass of the two atoms. The sum over squares of the lattice frequencies (ω^2) consists of six terms, at arbitrary wave vector $\mathbf{k}$, one term from each branch of the phonon spectrum. The rule has been shown to hold for the major lattice forces, called "trace constant" forces by Rosenstock.[13] Departures from constancy then throw light on "trace variable" forces, of which the most important are probably due to next-nearest neighbors.[13]

The sum rule was derived only for lattices of sufficient symmetry, the zincblende structure being one.[65] It is tempting to disregard this restriction, and to extend the rule to all wave vectors in all SiC polytypes, for $\bar{M}$ is always the same, and there is no significant variation in r_0. We therefore make the following three assumptions. (1) The compressibility of all polytypes can be represented by a single constant β. (2) The coefficient a is approximately independent of polytype structure. (3) The lattice forces do not depend significantly on the stacking order in polytypes, hence the appropriate large zone can be used for each polytype. This restricts the lattice sum to six terms, regardless of the number of atoms per unit cell.

For the principal phonons previously reported for several SiC polytypes, the extended sum rule appears to be valid, but of little interest, since there were only minor differences in the phonon spectra.[66] However, the 2*H* spectrum shows significant phonon differences, as indicated in Table IV, which gives phonon energies[67]

TABLE IV. Lattice frequencies and lattice sums for 2*H* and cubic SiC. The frequency ω is in units of 10^{14} rad/sec, and ω^2 in units of 10^{28} rad^2/sec^2.

Phonon	2*H* $\omega(K)$	2*H* $\omega^2(K)$	Cubic $\omega(X)$	Cubic $\omega^2(X)$	Cubic or 6*H* $\omega(0)$	Cubic or 6*H* $\omega^2(0)$
TA_1	0.80	0.64	0.70	0.49		
TA_2	0.94	0.88	0.70	0.49		
LA	0.94	0.88	1.21	1.46		
TO_1	1.39	1.93	1.43	2.04	1.49	2.23
TO_2	1.57	2.47	1.43	2.04	1.49	2.23
LO	1.52	2.31	1.56	2.43	1.84	3.39
Σ		9.11		8.95		7.85
$\Sigma(k)/\Sigma(0)$		1.16		1.14		

and lattice sums Σ for 2*H* and cubic SiC at their conduction band minima.[68] The comparison of $\Sigma(K)$ for 2*H* and $\Sigma(X)$ for cubic shows that these sums differ by less than 2%.

The last column of Table IV gives phonon frequencies at $\mathbf{k}=0$. The TO value is obtained from infrared measurements by Spitzer *et al.*, who found essentially the same resonance frequency for both cubic[69] and 6*H* SiC,[70] a result consistent with the proposed extension of the sum rule. The LO frequency has been obtained by use of the Lyddane-Sachs-Teller relation,[71] with dielectric constant of 10.2 at low frequencies,[72] and 6.7 in the optical region.[70]

[60] Lines in Fig. 1 of Ref. 7.

[61] The intensity ratio of primed to unprimed lines appears to be constant for $E\|c$, but not for $E\perp c$. Without knowledge of the mechanism involved, it can be seen that such a result might follow if recombination proceeds primarily through a single intermediate state for $E\|c$. In this case the transition would involve either electron scattering or hole scattering, but not both.

[62] J. L. Birman, Phys. Rev. **115**, 1493 (1959); J. J. Hopfield, J. Phys. Chem. Solids **15**, 97 (1960); M. Cardona, *ibid.* **24**, 1543 (1963).

[63] M. Cardona, Phys. Rev. **129**, 1068 (1963); **137**, A1467 (1965).

[64] E. Gutsche, Phys. Status Solidi **1**, 147 (1961); D. Berlincourt, J. Jaffe, and L. R. Shiozawa, Phys. Rev. **129**, 1009 (1963).

[65] S. S. Mitra and R. Marshall, J. Chem. Phys. **41**, 3158 (1964).

[66] Five other polytypes are known to have principal phonon energies that are close to those of cubic SiC. See Ref. 4, Table IV, and Ref. 7, Table I.

[67] In this section we give SiC phonon energies in rad/sec in order to facilitate comparisons with numerical values of lattice sums for other materials quoted in the references. 1 meV=1.52 $\times 10^{12}$ rad/sec.

[68] We have counted line 2 (61.5 meV) twice, as suggested by the discussion of Sec. VI A. However, taking the line *c* for the missing acoustic phonon would change the lattice sum by less than 1%.

[69] W. G. Spitzer, D. A. Kleinman, and C. J. Frosch, Phys. Rev. **113**, 133 (1959).

[70] W. G. Spitzer, D. A. Kleinman, and D. Walsh, Phys. Rev. **113**, 127 (1959).

[71] R. H. Lyddane, R. G. Sachs, and E. Teller, Phys. Rev. **59**, 673 (1941).

[72] D. Hofman, J. A. Lely, and J. Volger, Physica **23**, 236 (1957).

If it is valid to extend the sum rule to all polytypes it is meaningful to form lattice sum ratios $\Sigma(\mathbf{k})/\Sigma(0)$, even though numerator and denominator refer to different polytypes. The departure from unity of this ratio, shown in the last row of Table IV, gives a measure of the strength of the trace variable forces. The dependence of these forces on $\mathbf{k}$ has been discussed and illustrated by Rosenstock,[13] who shows that second neighbors probably make the largest contribution.

It is also of interest to compare lattice properties of SiC with those of Si and C (diamond). Neutron scattering results show that the phonon dispersion curves of Ge and Si differ mainly in scale,[73] but that diamond is quite dissimilar.[74] From the ratios $\Sigma(X)/\Sigma(0)$, Rosenstock has deduced that trace variable forces are negligible in Ge and Si, but quite important in diamond. Although the SiC data are limited, in the absence of neutron scattering results, the ratio $\Sigma(X)/\Sigma(0)$ is known (1.14 in Table IV) and may be compared with the values of unity for Ge and Si,[13] and 1.22 for diamond.[74] Thus, SiC falls between Si and diamond in the importance of trace variable forces, but is somewhat closer to diamond.

ACKNOWLEDGMENTS

We wish to thank M. M. Sopira, Jr., and N. R. Anderson for technical assistance.

APPENDIX: CRYSTAL GROWTH

Crystals of 2*H* SiC were grown by the reduction of methyltrichlorosilane after the fashion of Adamsky and Merz.[1] The crystals were grown on spectrographically pure graphite crucibles, 1 in. diam and 4 in. high, heated inductively within an insulated quartz reaction tube attached to a stainless-steel system which, when evacuated, was tight to a helium leak detector. Teflon seals were used throughout. Temperature was controlled to $\pm 1°C$, and optically measured in cavities within the crucible. In a typical experiment the crucible was outgassed at 1400°C overnight in a vacuum of 5×10^{-5} Torr. Hydrogen was then admitted to give a linear gas velocity past the crucible of 0.9 to 1.8 cm/sec. A small part of this stream was passed over the surface of liquid silane in a saturator, thermostated to obtain a final silane concentration of 0.4 to 0.8 mole %. A very uniform rate of delivery as well as the purification of a single stage of distillation was obtained this way. To help remove dissolved impurities, the silane itself was washed with hydrogen by bubbling prior to a run. It was also frozen with liquid nitrogen and pumped to eliminate foreign gases. Crystal growth times were typically 24 h.

Under these conditions, about 80% of the silicon in the silane was recovered as pure SiC on the crucible, the actual yield rising somewhat with operating temperature and with falling gas velocity. The majority of deposit was cubic SiC. At substrate temperatures below 1350°C, the crystallite size was vanishingly small. Between this temperature and 1430°C, some 2*H* crystals could usually be grown in each run. The number and size of these did not, however, correlate with any controlled parameters. Above 1430°C the crystals were almost entirely cubic. The fraction of 2*H* did depend upon the condition of inside wall of the initially transparent quartz tube, and rose appreciably when this became clouded or opaque because of reactant deposits or chemical attack. It is probable that the temperature gradient in the gas is important, but 2*H* growth did not respond in experiments in which this was deliberately altered.

The 2*H* morphology differed somewhat from that described by Adamsky and Merz,[1] for our crystals were usually tapered. The greatest difference, however, was in the purity, for many of the crystals were entirely transparent and colorless. The smaller whiskers and rods frequently nucleated and grew from a common site in a spherulitic deposit, a tendency which was prevalent at the lower substrate temperatures. To see if this behavior was caused by some local impurity in the crucible, Cr, Al, Fe, Co, Cu, Si, and Au spots were evaporated onto the graphite in separate experiments. The number of spherulites increased in almost every case, but the size of the crystals dropped. The largest crystals always grew singly.

It has been suggested[16] that SiC may grow by a vapor-liquid-solid (VLS) mechanism, for 2*H* whiskers often have balls attached to them which could be solidified solvent. Since many of the elements used above would be suitable solvents for a VLS mechanism, the whiskers and balls in all the experiments were examined. When the ball deposit occurred on the straight section of a whisker, it was found that the whisker was continuous through the ball, usually without any change in diameter, so the ball deposit was incidental to whisker growth. If the direction of the whisker growth changed at a ball, the initial whisker usually tapered sharply to a point within the ball, and the new growth started elsewhere on the ball surface, tapering slightly and growing in an unrelated direction. This habit was extremely common, often with as many as ten or fifteen changes of direction in a single strand. The strands almost always ended with a fine tipped whisker free of any ball deposit. The balls were for the most part cubic SiC,[1] but electron microprobe measurements could not rule out the possibility of a small

[73] B. N. Brockhouse and P. K. Iyengar, Phys. Rev. **111**, 747 (1958); B. N. Brockhouse, Phys. Rev. Letters **2**, 256 (1959).

[74] J. L. Yarnell, J. L. Warren, and R. G. Wenzel, Phys. Rev. Letters **13**, 13 (1964); Symposium on the Inelastic Scattering of Neutrons, Bombay, 1964 (International Atomic Energy Agency, to be published).

excess of Si. The incidence of balls decreased when metallic solvents, including Si, were deliberately added, and this, coupled with the morphological observations, suggests that the balls were incidental to the 2*H* whisker growth mechanism. In fact, it would appear that nucleation of cubic SiC and subsequent formation of a ball on the tip of a 2*H* crystal very likely stops whisker growth. This is borne out by the observation that the short whiskers usually ended with a ball, whereas the longest whiskers were always free of ball terminations. Thus, the VLS mechanism does not appear to provide an explanation of our observations.

PHYSICAL REVIEW VOLUME 143, NUMBER 2 MARCH 1966

Fundamental Optical Absorption in SnS_2 and $SnSe_2$*

G. Domingo,† R. S. Itoga, and C. R. Kannewurf
Department of Electrical Engineering, Northwestern University, Evanston, Illinois
(Received 12 August 1965; revised manuscript received 10 November 1965)

Optical absorption in single-crystal *n*-type SnS_2 and $SnSe_2$ has been studied at 300°K throughout the wavelength range 0.26 to 6.5 μ. Samples suitable for optical measurements were prepared by various vapor-deposition techniques. The electrical characteristics of the samples used in the absorption measurements were as follows: for $SnSe_2$, conductivity 3.6 $(\Omega\ \text{cm})^{-1}$, electron concentration 10^{18} per cm^3, mobility 27 $\text{cm}^2/\text{V sec}$; and for SnS_2, conductivity 10^{-7} $(\Omega\ \text{cm})^{-1}$. From transmittance and reflectance measurements, the absorption coefficient and index of refraction were determined for light polarized perpendicular to the crystallographic symmetry axis. From an analysis of the data in the high-absorption region, direct-transition band gaps of 1.62 and 2.88 eV were found for $SnSe_2$ and SnS_2, respectively. A threshold for possible indirect phonon-assisted transitions was found to occur at 0.97 eV for $SnSe_2$ and at 2.07 eV for SnS_2. Photoconductivity data for SnS_2 are also presented.

INTRODUCTION

RECENT studies of the various physical properties of the tin chalcogenide system have been chiefly concerned with the $Sn(X)$-type compounds. Very little information is now available concerning the physical properties of the anisotropic compounds of the type $Sn(X)_2$, in particular, for properites of SnS_2 and $SnSe_2$. Mooser and Pearson[1] predicted that $SnSe_2$ would exhibit semiconductor behavior. Busch *et al.*[2] verified this prediction from conductivity, Hall effect, and thermoelectric measurements. Similar results were obtained by Asanabe[3] from conductivity and Hall measurements. Electrical measurements for SnS_2 have not been reported.

Both SnS_2 and $SnSe_2$ belong to the hexagonal-CdI_2-structure type (designated the *C*6 type in *Strukturbericht*). The characteristic layer-type growth of the materials crystallizing in this system has made it possible to prepare excellent single-crystal specimens which have suitable geometry for optical measurements. The other principal compound of the $Sn(X)_2$-type chalcogenides, SnO_2, crystallizes in the tetragonal rutile-type structure. Recent optical studies of SnO_2 have been reported in two papers by Summitt *et al.*[4,5] In view of the limited information available in the literature for SnS_2 and $SnSe_2$, it seemed desirable to study additional properties by optical techniques especially since such measurements have not as yet been reported for these *C*6-type semiconductors.

EXPERIMENTAL

Polycrystalline ingots of SnS_2 and $SnSe_2$ were prepared by melting stoichiometric amounts of the component materials[6] in evacuated quartz tubes. In the case of SnS_2 which has a melting point at approximately 870°C, a 3-mm wall tubing was employed, since at this temperature the vapor pressure of sulfur is over 40 atm. The entire synthesis tube was encased in a stainless steel bomb for further explosion protection. The temperature was increased slowly over a 24-h period to 950°C, held constant for 72 h, and then allowed to slow cool to room temperature. In all preparation trials inspection of the ingot showed some evidence of an incomplete reaction with traces of SnS and unreacted sulfur still present in the tube.

* This research was supported by the Advanced Research Projects Agency of the Department of Defense through the Northwestern University Materials Research Center.
† Present address: Northrup Institute of Technology, Inglewood, California.
[1] E. Mooser and W. B. Pearson, Phys. Rev. **101**, 492 (1956).
[2] G. Busch, C. Frohlich, and F. Hulliger, Helv. Phys. Acta **34**, 359 (1961).
[3] S. Asanabe, J. Phys. Soc. Japan **16**, 1789 (1961).
[4] R. Summitt, J. A. Marley, and N. F. Borrelli, J. Phys. Chem. Solids **25**, 1465 (1964).
[5] R. Summitt and N. F. Borrelli, J. Phys. Chem. Solids **26**, 921 (1965).
[6] Sulfur and selenium were obtained from the American Smelting and Refining Company, purity: 0.99999+; tin from the Consolidated Mining and Smelting Company, of Canada, purity: 0.999999.